J. Fluid Mech. (1981), *vol.* 108, *pp.* 383–400
Printed in Great Britain

On the transition between regular and Mach reflection in truly non-stationary flows

By S. ITOH, N. OKAZAKI AND M. ITAYA

Department of Mechanical Engineering of
Kyushu Sangyo University, Fukuoka, Japan

(Received 7 February 1980)

Shock reflections over a convex and a concave wedge were investigated by using a 5×7 cm ordinary pressure-driven shock tube. Dry air was used for both the driving and driven gases. The large difference between the transition from regular (RR) to Mach reflection (MR) and that from MR to RR was observed, confirming the results obtained by Ben-Dor, Takayama & Kawauchi (1980). These results contradict all of the previous theoretical transition criteria. A new theory on the transition between RR and MR was developed by applying Whitham's 'ray shock' theory. This new theory agrees quite well with the experimental results.

1. Introduction

It is well known that when a travelling normal shock wave strikes a solid-wall boundary, it reflects in one of four configurations, that is, regular reflection (RR), single Mach reflection (SMR), complex Mach reflection (CMR), or double Mach reflection (DMR). Figure 1 shows the schematic diagram of reflection in pseudo-steady flows. In such flows, each of these reflections maintains a constant shock configuration increasing linearly with time from the instant the shock wave strikes the leading edge of the wedge. RR and SMR are characterized by two and three shock configurations, respectively (figures 1*a*, *b*). CMR is characterized by a 'kinked' reflected shock wave shown in figure 1(*c*) by capital *K*. DMR has two reflected shock waves, two Mach stems and two slip streams. Owing to the geometry of the model used to reflect oblique shock waves in a steady flow, CMR and DMR cannot be materialized, even though the flow behind the reflected shock wave can be supersonic (Ben-Dor & Glass 1978, 1979). Hence, only RR (figure 2*a*) and SMR (figure 2*b*) are possible.

When a travelling normal shock wave interacts with either a convex or concave wedge, there is a change in wedge angle θ_w causing the flow behind the reflected shock wave to become truly non-stationary. In truly non-stationary flow, the original reflection will change its configuration to RR or MR due to the gradual change of θ_w. Ben-Dor *et al.* (1980) have shown that there is a large difference between the angle of RR $\rightarrow$ MR transition and that of MR $\rightarrow$ RR transition. For example, at a Mach number of the incident shock wave $M_0 = 4$, the RR $\rightarrow$ MR transition occurred at $\theta_w \approx 40°$, while the MR $\rightarrow$ RR transition took place at $\theta_w \approx 65°$.

Three different theoretical transition criteria were reported by researchers in the years up to 1979. These were the 'detachment' criterion of von Neumann (1963); the

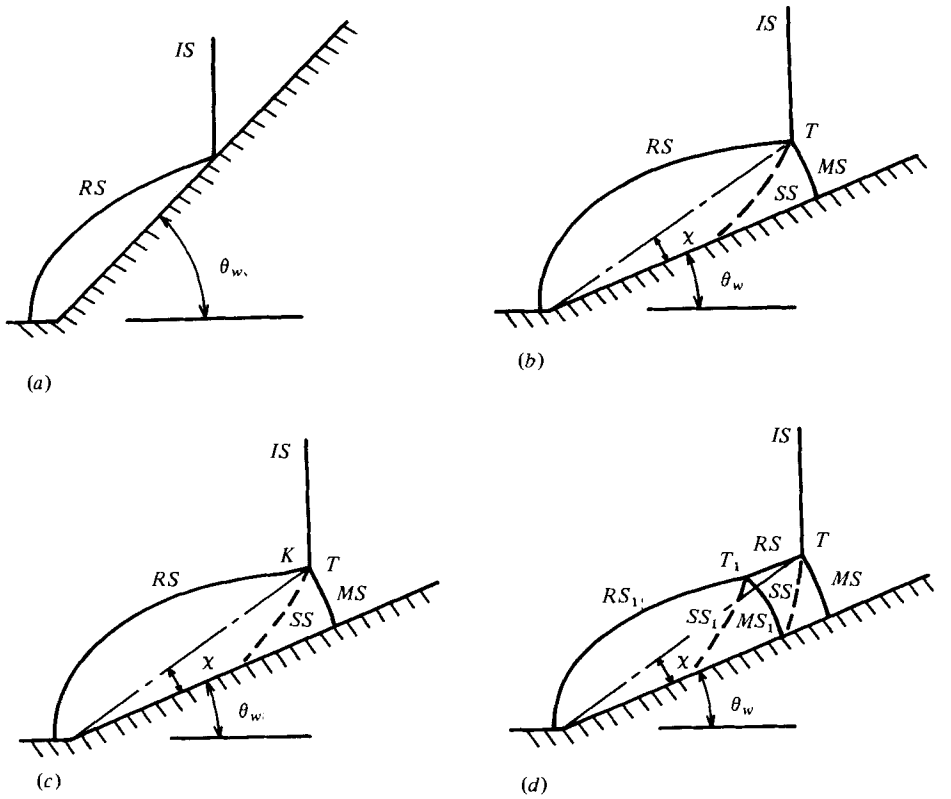

FIGURE 1. Illustration of four possible shock reflections in pseudo-steady flow. (*a*) Regular reflection (RR). (*b*) Single Mach reflection (SMR). (*c*) Complex Mach reflection (CMR). (*d*) Double Mach reflection (DMR). *IS*, incident shock wave; *RS*, RS_1, reflected shock wave; *MS*, MS_1, Mach stem; *SS*, SS_1, slip stream; *T*, T_1, triple points; χ, triple-point trajectory angle.

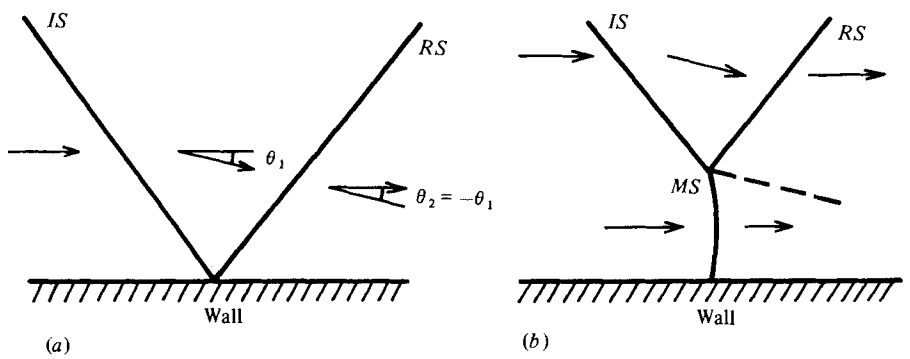

FIGURE 2. Schematic illustration of shock wave reflection in steady flows. (*a*) Regular reflection (RR): θ_1 and θ_2 are the deflection angles of flows across the *IS* and *RS*, respectively. (*b*) Single Mach reflection (SMR).

'mechanical-equilibrium' criterion of Henderson & Lozzi (1975); and the 'length-scale' criterion of Hornung, Oertel & Sandeman (1979). A full report dealing with these criteria and a comparison with experimental results was published by Ben-Dor *et al.* (1980). They believe that in steady flow, the RR $\rightleftarrows$ MR transition reduces to the 'mechanical-equilibrium' criterion of Henderson & Lozzi (1975). In pseudo-steady flows the transition could reduce to either Henderson & Lozzi's criterion *or* to von Neumann's 'detachment' criterion. But in truly non-stationary flows, the RR $\rightleftarrows$ MR transition does not reduce to any of previously reported criteria.

Heilig (1969) developed his theory of RR $\rightarrow$ MR transition by applying the 'ray shock' theory. Itoh & Itaya (1978) modified his theory by considering the strength of Mach stem (see subsequent discussion). The comparison between these theories and the experimental results was done by Ben-Dor *et al.* (1980). They have shown that Itoh & Itaya's theory is more accurate than Heilig's.

Until now there was no theoretical criterion for the MR $\rightarrow$ RR transition in truly non-stationary flows. Following is the outline of our theory on the RR $\rightarrow$ MR transition. Next we present a theory of MR $\rightarrow$ RR transition in truly non-stationary flow. Finally we compare this MR $\rightarrow$ RR transition theory to experimental results.

2. Analysis

The transition from RR to MR in truly non-stationary flows (outline)†

In shock wave reflection over a convex wedge, the RR $\rightarrow$ MR transition was observed at the critical angle. Although Heilig's theory was also developed by applying the 'ray shock' theory, there are many discrepancies between his theory and experimental results (Ben-Dor *et al.* 1980). Our theory was developed based on the experimental results shown in figure 3. This figure illustrates the shock wave system in the vicinity of the RR $\rightarrow$ MR transition point. From its geometry, we get the following equations for shock motion:

$$L = M_0 a_0 \delta t, \quad Ls = M_1 a_0 \delta t, \quad L' = Ls \,.\, \sin(\alpha_{\text{crit}}), \qquad (1a, b, c)$$

where a_0 is a sonic velocity at the undisturbed region ahead of the incident shock wave, M_1 is the Mach number of the Mach stem, and δt is an infinitesimal time. L and Ls are the distances through which IS and MS travel during δt. L' is the distance between IS and the intersection of the Mach stem and tangent $\overline{OZ}$. If L' becomes greater than L, we see the onset of Mach reflection. We therefore define the critical angle at which the Mach reflection occurs as

$$L' = L + 0, \quad \text{i.e.,} \quad M_1/M_0 \sin(\theta_{\text{crit}}) = \tan(\theta_{\text{crit}}) \qquad (2)$$

where $\theta_{\text{crit}} = \frac{1}{2}\pi - \alpha_{\text{crit}}$. As $\delta t \rightarrow 0$, M_1 may be estimated by the 'ray shock' theory, in the same way as with a straight wedge. Using the 'ray shock' theory, the strength of Mach stem at the wall angle of θ_w is found as follows:

$$\theta_w = \int_{M_0}^{M} \frac{dM}{\overline{AC}}, \qquad (3)$$

† Full report can be found in *J.S.M.E.* paper no. 396: 'On the transition from RR to MR', S. Itoh, I. Kambayashi & M. Itaya (1979).

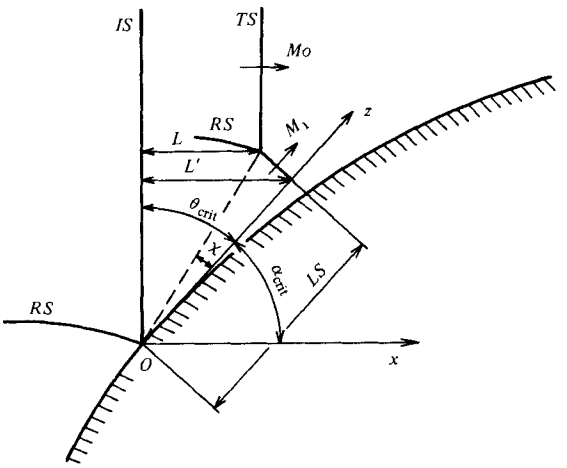

FIGURE 3. Schematic illustration of shock wave system in the vicinity of the transition point in RR → MR transition. α_{crit} is the critical incident angle at which the Mach reflection occurs. *TS* is the transmitted shock. *O* is the transition point.

where $A = A(M)$ and is an area of ray tube, M is the shock wave Mach number, and C is the characteristic velocity. The value of A is found using the following equation, known as the CCW equation (Chester 1954; Chisnell 1957; Whitham 1958):

$$\frac{dA}{A} = \frac{-2MdM}{(M^2-1)K(M)}, \tag{4}$$

where

$$K(M) = 2\left[\left(1+\frac{\gamma}{\gamma+1}\frac{1-\mu^2}{\mu}\right)(2\mu+1+M^{-2})\right]^{-1} \tag{5}$$

and

$$\mu^2 = \frac{(\gamma-1)M^2+2}{2\gamma M^2-(\gamma-1)}; \tag{6}$$

γ is the specific heat ratio. $K(M)$ is a slowly varying function which starts at 0·5 for weak shocks, when $M = 1$, and decreases to 0·394 (when $\gamma = 1{\cdot}4$) as $M \to \infty$.

Supposing that $K(M)$ is constant and equal to n, then the integration of (3) readily yields the next equation:

$$\frac{M_1}{M_0} = \frac{1}{2M_0}\{[(M_0^2-1)^{\frac{1}{2}}+M_0]\exp[(\tfrac{1}{2}n)^{\frac{1}{2}}\theta_w]+[(M_0^2-1)^{\frac{1}{2}}+M_0]\exp[(\tfrac{1}{2}n)^{\frac{1}{2}}\theta_w]^{-1}\}. \tag{7}$$

By the iterative numerical procedure, we get the value of M_1 for given θ_w and M_0.

In the extreme case of $M_0 \to 1$, (7) reduces to

$$M_1/M_0 = \cosh(\tfrac{1}{2}\theta_w). \tag{8}$$

By expanding (8) with θ_w and neglecting the higher order of θ_w^4, we get

$$M_1/M_0 = (1+\theta_w^2/8). \tag{9}$$

Equation (9) is the same as the original equation for weak shock wave given by Whitham (1957).

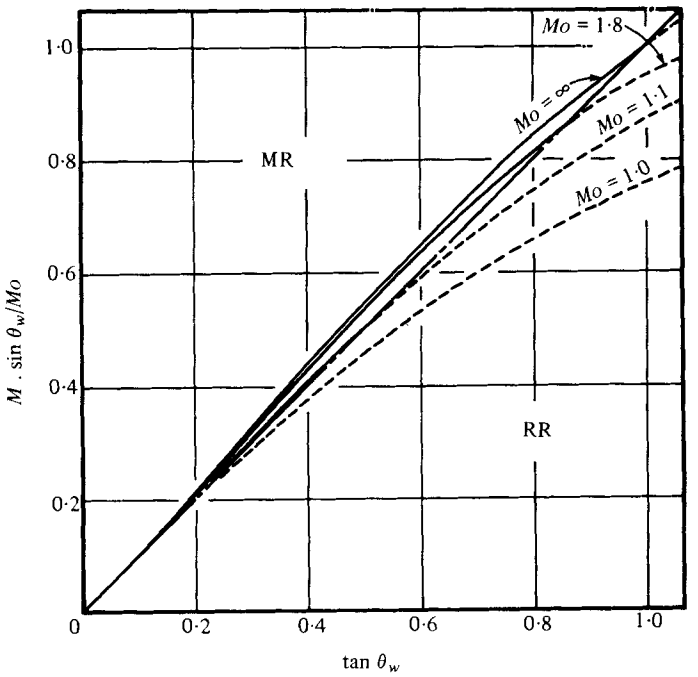

FIGURE 4. Graphs of the calculated values for $M_1 \sin(\theta_w)/M_0$ obtained using (11) versus $\tan\theta_w$. – – –, the straight line having a slope of 1 and dividing the regions of MR and RR. Using the values assigned to M_0 written on the respective lines: ——, the calculated values for $M_1 \sin(\theta_w)/M_0$ in the region of MR; – – –, the calculated values for $M_1 \sin(\theta_w)/M_0$ in the region of RR.

In the other extreme case of $M_0 \to \infty$, we get

$$M_1/M_0 = \exp[(0{\cdot}394/2)^{\frac{1}{2}}\theta_w]. \tag{10}$$

Equation (10) is the same as the original equation given for strong shock wave (Whitham 1957).

By substituting (7) for (2), we obtain the theory of transition from RR to MR as follows:

$$\frac{1}{2M_0}\{[(M_0^2-1)^{\frac{1}{2}}+M_0]\exp[(\tfrac{1}{2}n)^{\frac{1}{2}}\theta_w]+([(M_0^2-1)^{\frac{1}{2}}+M_0]\exp[(\tfrac{1}{2}n)^{\frac{1}{2}}\theta_w])^{-1}\}\sin\theta_w = \tan\theta_w. \tag{11}$$

In equation (11), θ_{crit} is replaced by θ_w in order to have a general meaning. We cannot get the solution of (11) analytically but iteratively. Some results of calculations are shown in figure 4. In this figure RR and MR indicate the regions where the regular and Mach reflections occur. The points of intersection between the straight and curved lines are the critical angles in RR $\to$ MR transition. The critical angles are shown in table 1. The angles θ_{ray} and θ_{det} indicate the theoretical critical angles obtained by (11) and by the 'detachment' criterion of von Neumann (1963), respectively; θ_{mech} indicates the theoretical critical angle obtained by the 'mechanical-equilibrium' criterion of Henderson & Lozzi (1975). ξ is the inverse pressure ratio of incident shock wave. When $\xi > 0{\cdot}433$, a value for θ_{mech} could not exist, as pointed out by both Kawamura & Saito (1956) and Henderson & Lozzi (1975). The critical angles obtained

ξ	θ_{ray}	θ_{det}	θ_{mech}
0·0	45·25	50·03	67·50
0·1	44·42	50·80	60·90
0·2	43·16	50·75	56·30
0·3	41·58	50·15	52·90
0·4	39·75	49·91	49·70
0·5	37·61	47·50	—
0·6	34·98	45·45	—
0·7	31·70	42·30	—
0·8	27·28	37·40	—
0·9	20·46	29·25	—
1·0	0·00	0·00	—

TABLE 1. Critical angle values in RR $\rightarrow$ MR transition. θ_{ray} and θ_{det} indicate the critical angles obtained using (11) and by the 'detachment' criterion of von Neumann (1963), respectively. θ_{mech} is the critical angles from Henderson & Lozzi's criterion.

by Hornung *et al.*'s 'length-scale' criterion were almost identical to the values of von Neumann's 'detachment' criterion in pseudo steady flows. Therefore, we eliminated the 'length-scale' criterion from this table.

The transition from MR to RR in truly non-stationary flows

Figure 5 shows the schlieren photograph of Mach reflection over the concave wedge. It was taken at the initial pressure $P_0 = 50$ torr, and the initial temperature $T_0 = 300$ K. τ indicates the time measured from the instant the travelling normal shock wave strikes the leading edge of the wedge. It can be seen that the Mach stem is almost straight and nearly perpendicular to the tangent of the concave wedge. A schematic diagram of MR over the concave wedge is shown in figure 6. Assuming that the Mach stem is straight and perpendicular to the tangent of the concave wedge, then the strength of Mach stem at any given instant will be the same at all points along itself. From the geometry of figure 6, we get the equations:

$$A_1 = \lambda, \quad A_0 = \cos\theta_0 - (1-\lambda)\cos(\theta_0+\phi); \tag{12a, b}$$

$$L = M_0 d\alpha_1 = [1-(\lambda+d\lambda)]\sin(\theta_0+\phi+d\phi) - (1-\lambda)\sin(\theta_0+\phi); \tag{13}$$

where L is a distance through which the incident shock wave travels during the infinitesimal time interval dt, and λ is an undimensionalized length of Mach stem. ϕ is the $\angle QON$ as shown in this figure. $d\lambda$ and $d\phi$ are infinitesimal increments of λ and of ϕ, respectively. θ_0 is the initial angle of a concave wedge. A_0 and A_1 are $A(M_0)$ and $A(M_1)$, respectively.

Supposing that both $d\lambda$ and $d\phi$ are much smaller than 1, then we may neglect their higher orders. By rearranging (13), we get the ordinary differential equation:

$$\frac{d\lambda}{d\phi} = \frac{1-\lambda}{\tan(\theta_0+\phi)} - \frac{M_0}{\sin(\theta_0+\phi)}\left(\frac{d\alpha_1}{d\phi}\right). \tag{14}$$

From Bryson & Gross (1961), we get the relation between $d\alpha_1 = a_0 dt$ and $d\phi$ as follows:

$$d\alpha_1/d\phi = (1-\tfrac{1}{2}\lambda)/M_1. \tag{15}$$

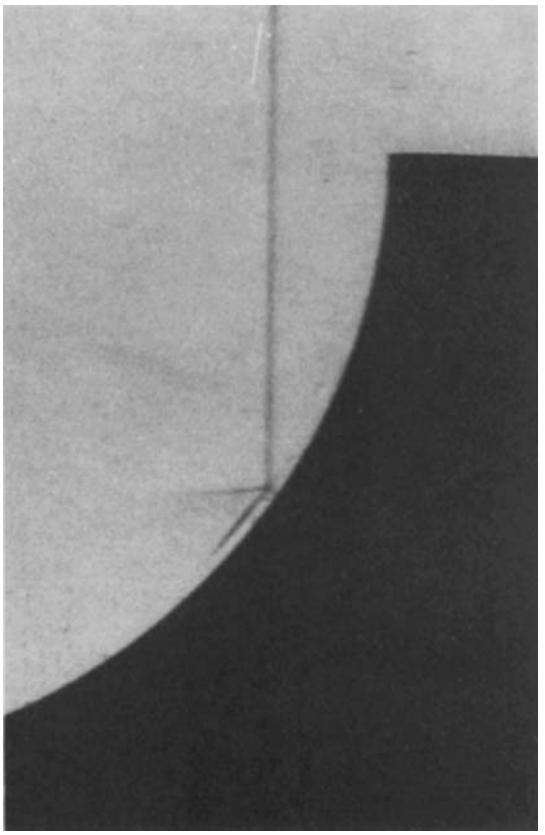

FIGURE 5. An instantaneous schlieren photograph of the Mach reflection over the concave wedge. $M_0 = 1{\cdot}8$, $\tau = 62{\cdot}18\ \mu$s, $P_0 = 50$ torr, $T_0 = 300$ K.

Substituting into (14), the equation for the length of Mach stem follows

$$\frac{d\lambda}{d\phi} = \frac{1-\lambda}{\tan(\theta_0+\phi)} - \frac{1-\lambda/2}{\sin(\theta_0+\phi)}\left(\frac{M_0}{M_1}\right). \tag{16}$$

In calculating the length of Mach stem using (16), the value of M_0/M_1 has to be estimated. Using the following expression for the characteristic velocity C:

$$C = [d(-M^2)/d(A^2)]^{\frac{1}{2}} \tag{17}$$

then (3) may be altered to

$$\theta_w = \int_{M_0}^{M}\left[-\frac{A^{-1}dA/dM}{M}\right]^{\frac{1}{2}} dM. \tag{18}$$

The relation between A and M described by (4) was deduced by neglecting the effects of the reflected shock wave and of the slip stream. Oshima *et al.* (1965) and Milton (1975) successfully added those effects. Milton's modification was made using the Rankine–Hugoniot condition at $M \to \infty$, which is only useful for a strong shock wave. We modified the relation between A and M using the full Rankine–Hugoniot condition which is useful for all shock wave strengths. The reflected shock wave and the slip stream deform C^+ as seen in figure 7(*b*) (Oshima *et al.* 1965; Milton 1975). This change is described by

$$(d\zeta)_1^2 = (d\zeta)_1^3 + (d\zeta)_3^2 \tag{19}$$

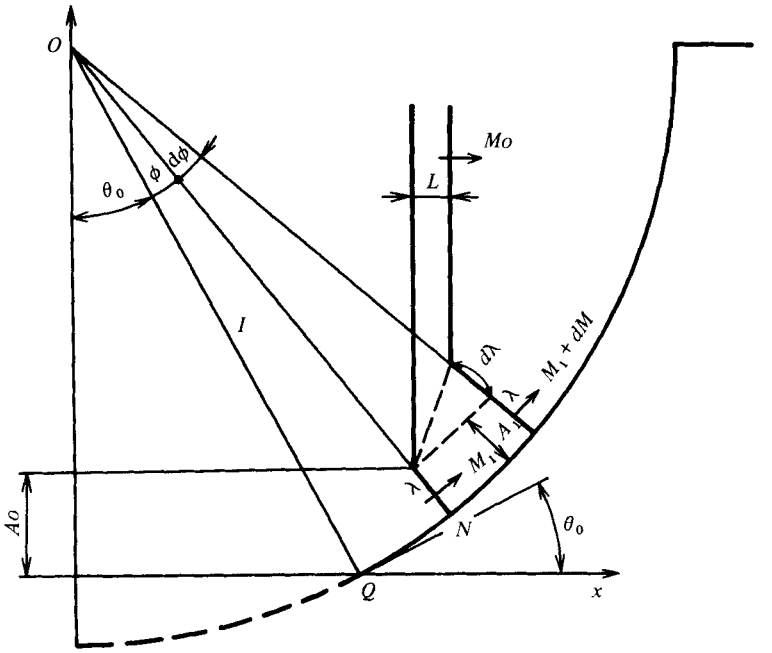

FIGURE 6. A schematic diagram of shock wave reflection over a concave wedge. O is the origin of the radius of the curvature of the concave wedge. Other notations are explained in the text.

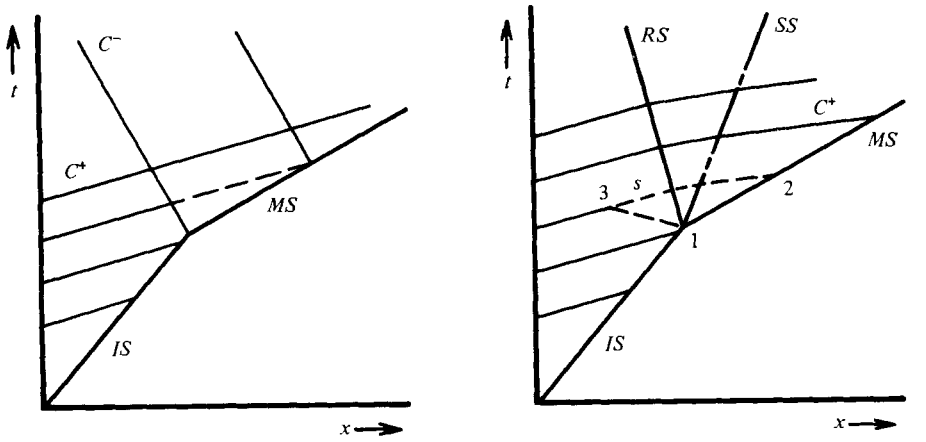

FIGURE 7. Schematic diagrams of x–t wave. (a) Non-disturbance case. (b) Single Mach reflection case. C^+ and C^- indicate the characteristic lines.

where $d\zeta = du + (dp/\rho) + [ua/(u+a)]d(\ln A)$, in which p is pressure, ρ is density and u is flow velocity. On line $\overline{31}$, the incident shock wave is undisturbed and du, dp and $d(\ln A)$ are all zero, making $(d\zeta)_1^3$ equal to zero. By integrating $d\zeta$ between the points 3 and 2, and differentiating with respect to s in the characteristic direction, a disturbance term follows

$$\frac{d}{ds}\int_3^2 d\zeta = \frac{d\zeta_2}{ds} - \frac{d\zeta_3}{ds} + \epsilon + \sigma, \tag{20}$$

where $$\epsilon = \int_3^2 \frac{\partial}{\partial s}\left(\frac{1}{\rho a}\right) dp, \quad \sigma = \int_3^2 \frac{\partial}{\partial s}\left(\frac{ua}{u+a}\right) d(\ln A).$$

Substituting into (19) gives the disturbed case:

$$(d\zeta)_1^2 - (\epsilon + \sigma)\, ds = 0. \tag{21}$$

Using the full Rankine–Hugoniot condition on the derivatives of correction terms $d\epsilon/dp$ and $d\sigma/d(\ln A)$, we get

$$\frac{d\epsilon}{dp} = \frac{-2}{\rho_0 a_0 M^2} \frac{2[2\gamma M^2 - (\gamma-1)] + (\gamma-1)(1+\gamma M^4)}{[2\gamma M^2 - (\gamma-1)]^{\frac{3}{2}} [(\gamma-1) M^2 + 2]^{\frac{1}{2}}} \frac{dM}{ds} \tag{22}$$

and

$$\begin{aligned} \frac{d\sigma}{d(\ln A)} = [2a_0\{&[2\gamma M^2 - (\gamma-1)]^{\frac{3}{2}} [(\gamma-1) M^2 + 2]^{\frac{3}{2}} (M^2+1) + 4(\gamma-1)(M^2-1)^2 \\ &\times (1+\gamma M^4)\}/\{(\gamma+1) M^2 [2\gamma M^2 - (\gamma-1)]^{\frac{1}{2}} [(\gamma-1) M^2 + 2]^{\frac{1}{2}} \\ &\times [2(M^2-1) + \{2\gamma M^2 - (\gamma-1)\}^{\frac{1}{2}} \{(\gamma-1) M^2 + 2\}^{\frac{1}{2}}]^2\}] \frac{dM}{ds}. \end{aligned} \tag{23}$$

Also using the full Rankine–Hugoniot condition on $(d\zeta)_1^2$, and combining the integrated forms of (22) and (23), we get the modified relation between A and M as follows:

$$\frac{dA}{A} = \frac{-2M\, dM}{(M^2-1) K(M)} - \frac{\eta}{M} dM, \tag{24}$$

where

$$\eta = \left(1 - \frac{M_0^2}{M^2}\right) \frac{(F+2B) E}{(M^2-1) BD} + \tfrac{1}{2} \ln\left(\frac{A_0}{A}\right) \frac{D^{\frac{3}{2}}(M^2+1) + 4(M^2-1)^2 F}{(M^2-1) DE} \tag{25}$$

and

$$B = 2\gamma M^2 - (\gamma-1), \quad C = (\gamma-1) M^2 + 2, \quad D = BC,$$

$$E = 2(M^2-1) + \sqrt{D}, \quad F = (\gamma-1)(1+\gamma M^4).$$

In the extreme case of $M_0 \to \infty$, η reduces to

$$\eta_\infty = \frac{1}{2\gamma}\left\{\left[\frac{\gamma(\gamma-1)}{2}\right]^{\frac{1}{2}} + 1\right\}\left(1 - \frac{M_0^2}{M^2}\right) + \tfrac{1}{2} \ln\left(\frac{A_0}{A}\right). \tag{26}$$

Equation (26) is the same equation obtained by Milton (1975).

Integrating in (4) and in (24), A is given by

either $$A = kf(M), \quad f(M) = \exp\left\{\int -\left[\frac{2M}{(M^2-1) K(M)}\right] dM\right\} \tag{27a}$$

or $$A = kf(M), \quad f(M) = \exp\left\{\int -\left[\frac{2M}{(M^2-1) K(M)} + \frac{\eta}{M}\right] dM\right\} \tag{27b}$$

where k is any arbitrary constant. The calculated values of $\log_{10} f(M)$ using either (27*a*) or (27*b*) are plotted in figure 8. As can be seen, use of the correction term significantly changes the relation of A–M.

Using the modified relation between A and M, θ_w is described as follows:

$$\theta_w = \int_{M_0}^{M} \left[\frac{2}{(M^2-1) K(M)} + \frac{\eta}{M^2}\right]^{\frac{1}{2}} dM. \tag{28}$$

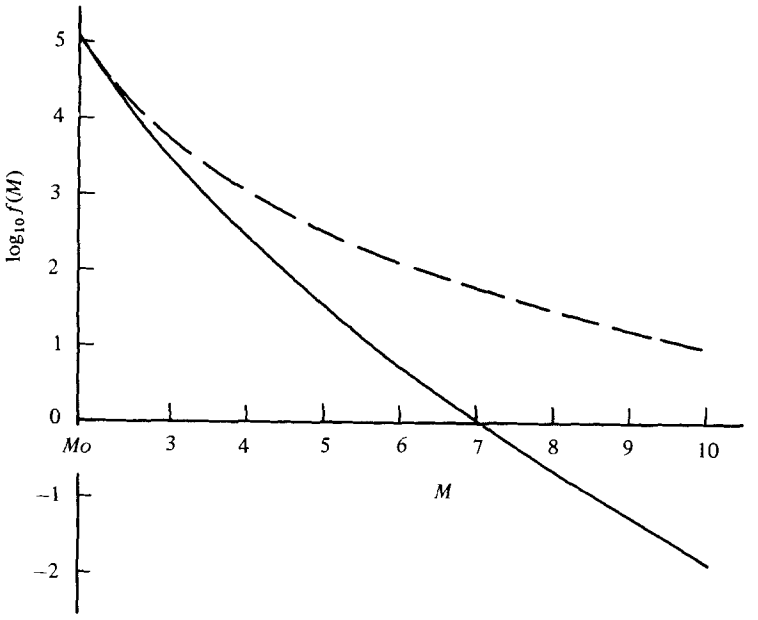

FIGURE 8. Graph of the values for $\log_{10} f(M)$ in the case $M_0 = 1{\cdot}8$. – – –, calculated values obtained using (27*a*); ——, calculated values obtained using (27*b*).

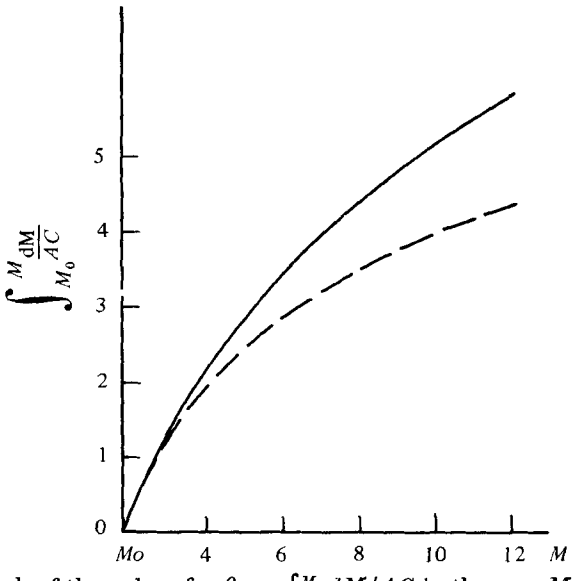

FIGURE 9. Graph of the values for $\theta_w = \int_{M_0}^{M} dM/AC$ in the case $M_0 = 1{\cdot}8$. – – –, calculated values obtained using (28); ——, calculated values obtained using (18).

The calculated values for θ_w obtained using (28), are shown in figure 9, together with those obtained by (18). As M increases, the values of θ_w obtained using (28) increase more steeply than those obtained using (18).

In calculating the length of Mach stem using both (16) and (28), we used the initial value of λ_0 at the angle $\phi_0 = 0{\cdot}5°$. λ_0 was given by the distance between the points I

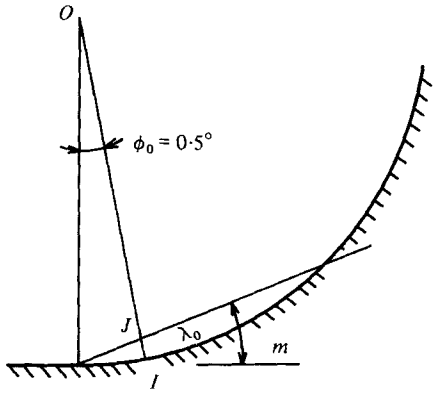

FIGURE 10. Illustration of the way in which the initial length of Mach stem λ_0 is determined. The notations are explained in the text.

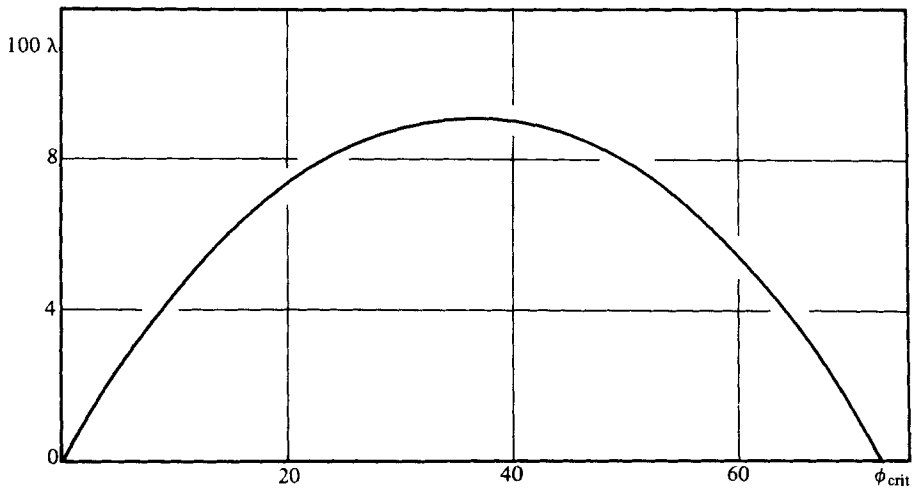

FIGURE 11. The calculated length of Mach stem in the concave wedge at strong incident shock strength ($M_0 \to \infty$) using (16) with (28).

and J shown in figure 10. The point I exists on the concave wedge. The point O is the origin of the radius of the curvature of the concave wedge. The line $\overline{OI}$ is perpendicular to the tangent of the concave wedge. J is the point of intersection between the line $\overline{OI}$ and the line having a slope of $\tan m$ originating from the leading edge of the concave wedge. The term of m indicates the characteristic angle defined as

$$\tan m = \left[\frac{(M^2-1)\,K(M)}{2M^2}\right]^{\frac{1}{2}}. \tag{29}$$

Figure 11 shows the calculated results obtained in the case of $M_0 \to \infty$. $\lambda_0 = 0{\cdot}003812$, $m = 23{\cdot}938°$ and $\phi_{crit} = 72{\cdot}5°$. As ϕ increases, λ also increases from λ_0 to its maximum, then it decreases continuously to zero at ϕ_{crit}. We define ϕ_{crit} as the critical angle of the MR $\to$ RR transition in truly non-stationary flows.

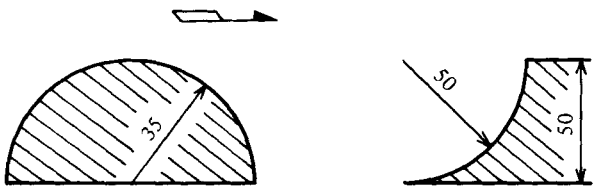

(a) (b)

FIGURE 12. Scale drawings of the two models used in the present study. (a) Model A, convex wedge. (b) Model B, concave wedge.

3. Experiments

The experiments were carried out using an ordinary pressure driven shock tube with a 5×7 cm rectangular duct. This was constructed from structural steel duct and consisted of a 1·62 m driver and a 5 m driven section followed by a test section. Mylar plastic sheet was used as the diaphragm material. The incident shock wave Mach number tested was $1{\cdot}15 \leqslant M_0 \leqslant 2{\cdot}0$. The shock wave velocity was measured with a digital counter and pressure transducers located 300 mm apart just ahead of the test section. Dry air was used for the driver and driven gases. The initial temperature T_0 was about 300 K in all the tests. The initial pressure P_0 was varied from 10 to 300 torr in order to change the strength of the incident shock wave. A semicylinder having a radius of 35 mm (model A, figure 12a) and a quadrant block with a radius of 50 mm (model B, figure 12b) were used for the convex and the concave wedges, respectively. Photographic studies were carried out using a time-delayed spark schlieren optical system triggered by a pressure transducer located just ahead of the test section. With this test arrangement only one photograph could be obtained for each firing of the shock tube, so that the sequence of events over the models A and B was pieced together from the results of several separate runs. Test conditions for each run were observed to be satisfactory for accuracy.

4. Results and discussion

A series of schlieren photographs obtained using the models A and B are shown in figures 13 and 14, respectively. In both cases, the incident shock wave is moving from left to right. As τ, defined previously, increases, there is the transition from RR (figure 13a) to MR (figure 13c) with model A. With model B, as τ increases, there is the transition from MR (figure 14a) to RR (figure 14c).

Figure 15 shows the locus of triple points, defined as the point of intersection of three shock waves – the reflected shock wave, the Mach stem and the incident shock wave. α_{ray} and α_{det}, respectively, are complementary angles of θ_{ray} and θ_{det}. The points G_A and G_B are located on the convex wedge, and were found using the critical angle obtained from (11) and by the 'detachment' criterion, respectively. Lines A and B, originating from the points G_A and G_B, respectively, were drawn by the method of characteristic (Bryson & Gross 1961). Line A is in better agreement with the experimental results than line B.

Actual Mach stem lengths are shown in figure 16 compared to the graphs of theoretical calculation. A solid and a broken line indicate the theoretical lengths of Mach stem

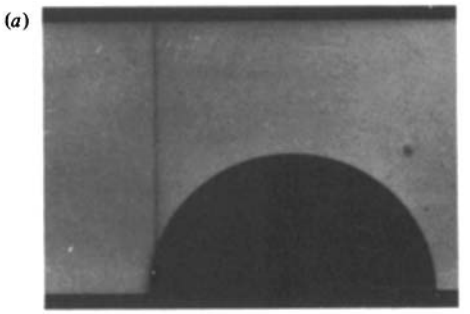

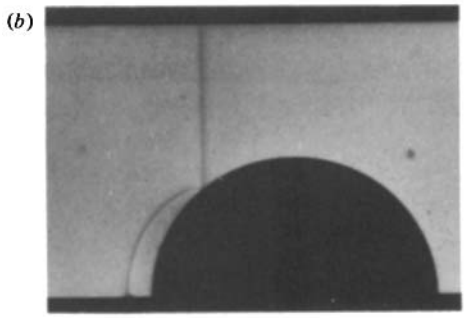

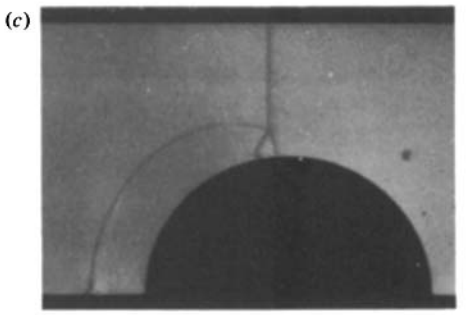

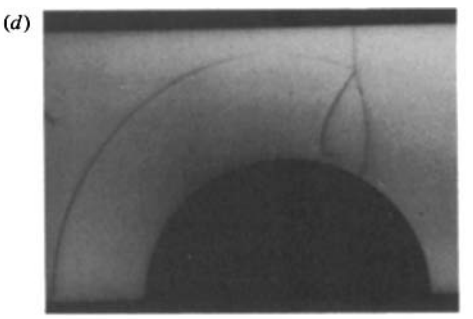

FIGURE 13.

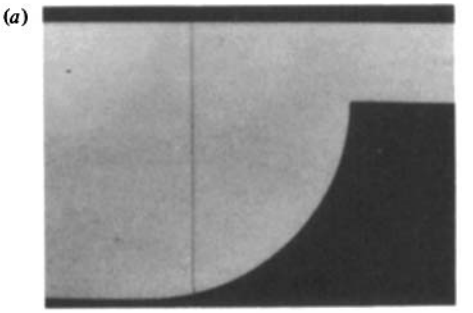

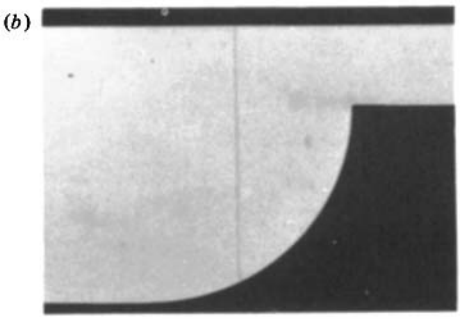

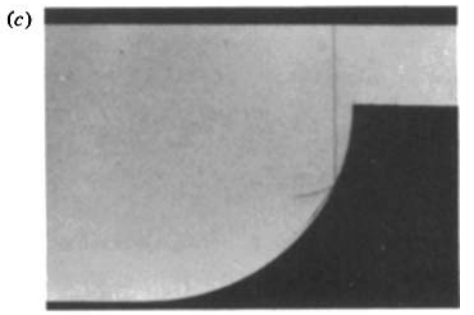

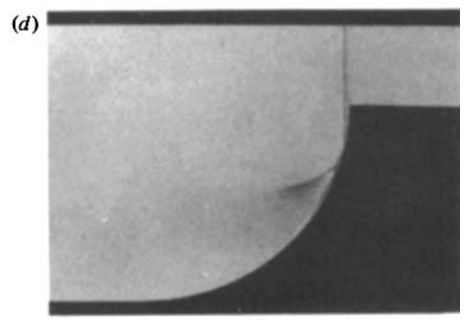

FIGURE 14.

FIGURE 13. A series of schlieren photographs. Shock-wave reflection over the convex wedge (model *A*) when $M_0 = 1{\cdot}8$. (*a*) $\tau = 7{\cdot}85\ \mu$s, (*b*) $24{\cdot}43\ \mu$s, (*c*) $50{\cdot}01\ \mu$s, (*d*) $89{\cdot}79\ \mu$s.

FIGURE 14. A series of schlieren photographs. Shock-wave reflection over the concave wedge (model *B*) when $M_0 = 1{\cdot}8$. (*a*) $\tau = 18{\cdot}14\ \mu$s, (*b*) $35{\cdot}96\ \mu$s, (*c*) $\tau = 74{\cdot}30\ \mu$s, (*d*) $79{\cdot}93\ \mu$s.

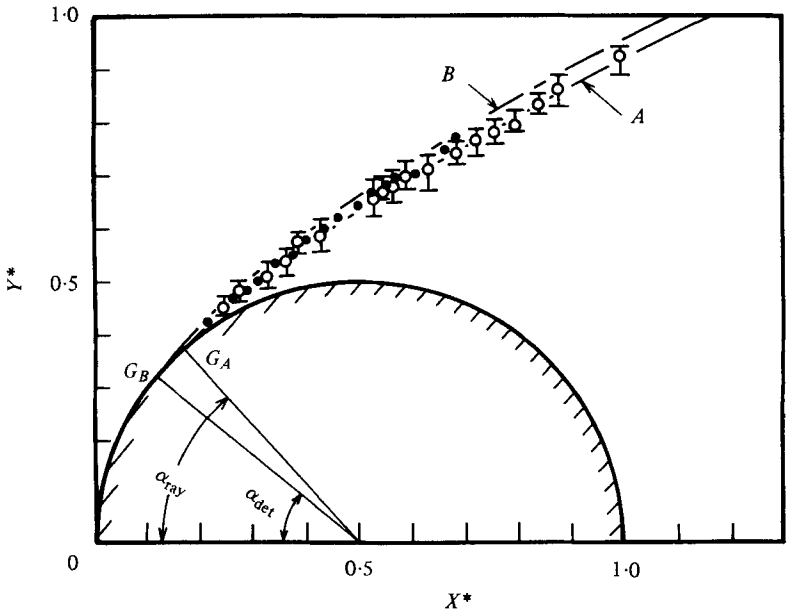

FIGURE 15. The locus of triple points in shock wave reflection over the convex wedge when $M_0 = 1{\cdot}92$. ⊖, our experimental results; ●, Heilig's data (1969); line A, the theoretical locus of triple points originating at G_A; line B, the theoretical locus of triple points originating at G_B.

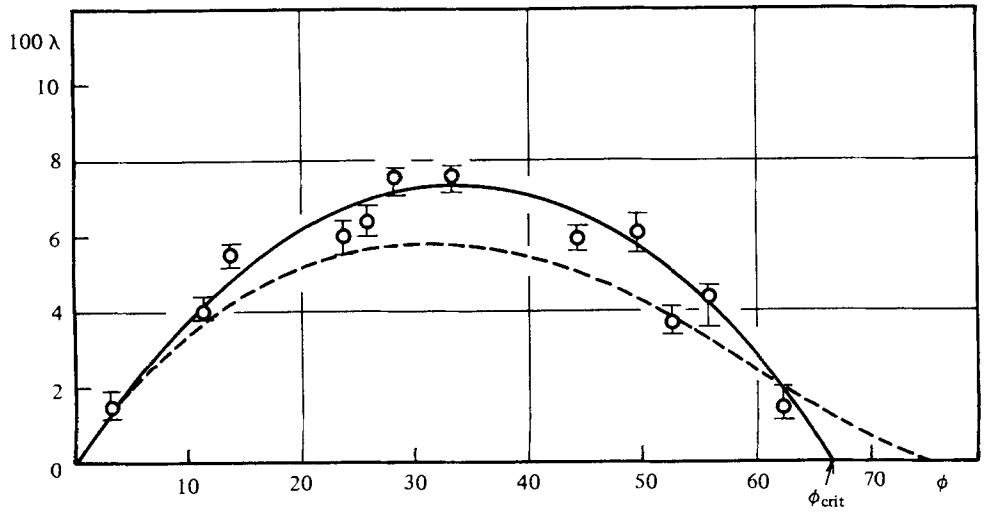

FIGURE 16. The length of Mach stem in Mach reflection over the concave wedge when $M_0 = 1{\cdot}8$. ⊖, experimental results; ——, the calculated length of Mach stem obtained using (16) with (28); – – –, the calculated length of Mach stem obtained using (16) and (18).

obtained using (16) with (28) and with (18), respectively. ϕ_{crit} is the angle at which the theoretical length of Mach stem, obtained using (16) with (28), becomes zero. As previously stated, we define ϕ_{crit} as the critical angle of the MR → RR transition in truly non-stationary flows. We see that the theoretical lengths of Mach stem indicated by the solid line, are in better agreement with the experimental results than those indicated by the broken line. Also, the theoretical critical angles of MR → RR tran-

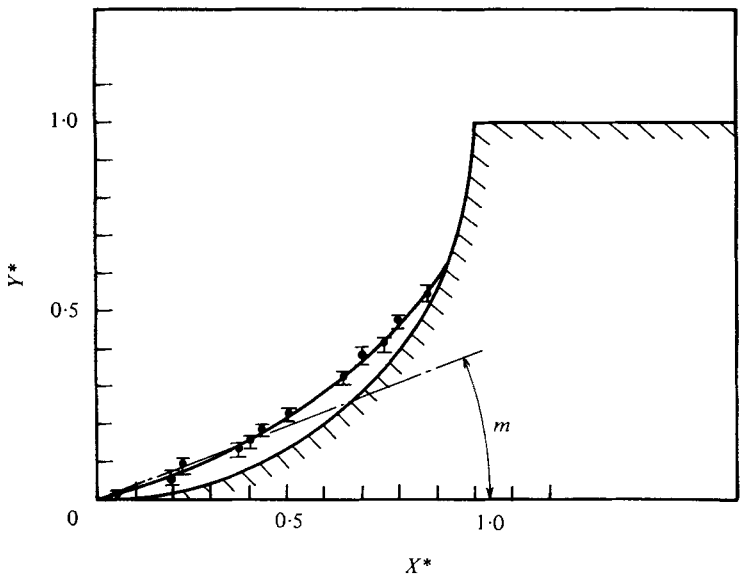

FIGURE 17. The locus of triple points in shock wave reflection over the concave wedge when $M_0 = 1{\cdot}8$. ⧫, experimental results; — – —, the straight line having a slope of tan m originating from the leading edge of the concave wedge; ——, the calculated locus of triple points obtained using (16) with (28).

sition (ϕ_{crit}) are very close to those found in experiments. Using the theoretical lengths of Mach stem, we can draw the locus of triple points over the concave wedge. An example ($M_0 = 1{\cdot}8$) can be seen in figure 17. The solid line indicates the theoretical locus of triple points obtained using (16) with (28). Near the leading edge of the concave wedge, the experimentally found locus of triple points is very close to the straight line having a slope of tan m. This evidence proves the assumption that λ_0 can be found by the method used for figure 11. We see that the theory matches well with the experimental results.

The comparison between the theoretical and experimental critical angles of the MR $\rightleftarrows$ RR transition is shown in figure 18. Lines I and II indicate the theoretical critical angles obtained by Henderson & Lozzi's criterion (1975), and by the 'detachment' criterion of von Neumann (1963), respectively. Line III indicates the theoretical critical angle obtained by (11). Line IV indicates the theoretical critical angle obtained using (16) with (28). The symbol ⧩ indicates the experimental results of Heilig (1969) obtained when the reflection of a shock wave is over a convex wedge. The symbols □ and ■ indicate the experimental results of Ben-Dor *et al.* (1980) obtained from the shock wave reflection over a convex and a concave wedge, respectively. Our experimental results are shown using ⧖ for reflection over a convex wedge, and ⧫ for reflection over a concave wedge. All of the experimental critical angles of the RR $\rightleftarrows$ MR transition in truly non-stationary flows were very different from theoretically calculated angles indicated by lines I and II. In the RR $\rightarrow$ MR transition, line III agrees quite well with the experimental results up to the strong shock strength of $\xi \approx 0{\cdot}6$. When $\xi < 0{\cdot}6$, the discrepancies between line III and the experimental results increase as ξ decreases. This may be explained by not accounting for real gas effects and the disturbances occurring behind the Mach stem. The difference between

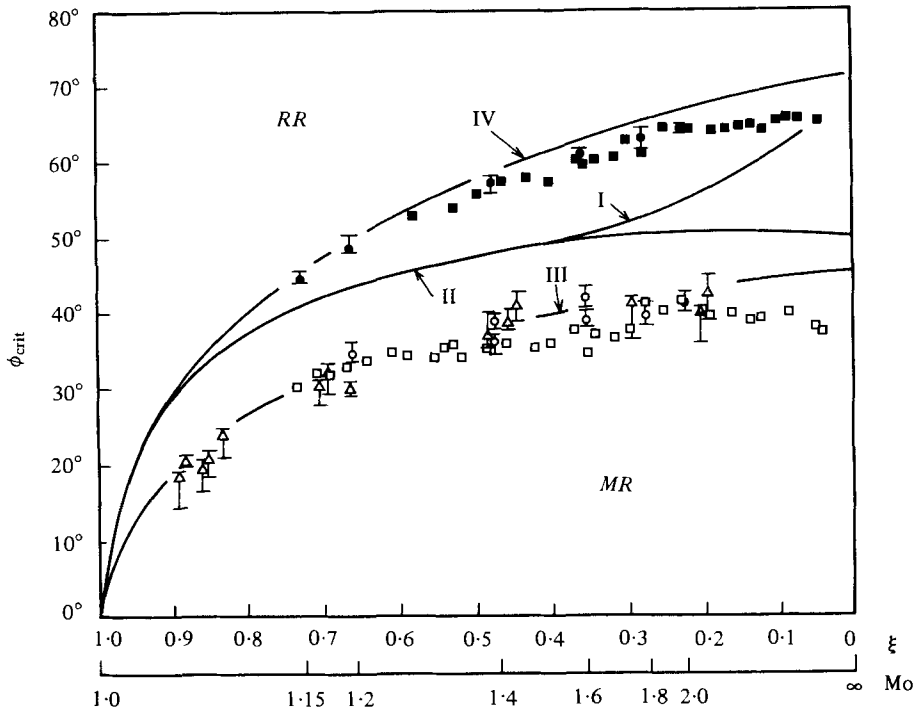

FIGURE 18. Experimental results of the MR → RR and RR → MR transition in the $(\xi - \phi_{crit})$ plane and some theoretical transition lines. ϕ_{crit} is the critical angle of the MR → RR or RR → MR transition. ξ is the inverse pressure ratio across the incident shock wave. □, Ben-Dor *et al.*'s data (1980) over the convex wedge; △, Heilig's data (1969) over the convex wedge; ○, our results over the convex wedge; ■, Ben-Dor *et al.*'s data (1980) over the concave wedge; ●, our experimental results over the concave wedge. Line I is the transition according to the 'mechanical-equilibrium' criterion of Henderson & Lozzi (1975). Line II is the transition according to the 'detachment' criterion of von Neumann (1963). Line III is the transition obtained by (11). Line IV is the transition obtained by (16) with (28).

the critical angle of RR → MR transition and that of MR → RR transition in truly non-stationary flows is reconfirmed by our tests. A new theory indicated by line IV agrees quite well with the experimental results of MR → RR transition up to $\xi \approx 0{\cdot}5$. When $\xi < 0{\cdot}5$, the discrepancies between line IV and the experimental results increase as ξ decreases. This, again, may be explained by not accounting for real gas effects and the disturbances occurring behind the Mach stem. The disturbances occurring behind the Mach stem, as pointed out by Milton (1975), may deform the Mach stem. The strength of Mach stem, therefore, cannot be determined by (7), nor can it be assumed that the strength of Mach stem at any given instant is the same at all points along itself.

5. Conclusion

Our experiments revealed that the transition from RR to MR and that of MR to RR are clearly different in truly non-stationary flows. The experiments also indicated that, in truly non-stationary flows, the critical angles of the RR ⇄ MR transition

contradict all of the previous transition criteria, that is, the 'detachment' criterion of von Neumann (1963); the 'mechanical-equilibrium' criterion of Henderson & Lozzi (1975); and the 'length-scale' criterion of Hornung *et al.* (1979).

Our theory of the critical angles of RR → MR transition was developed by applying Whitham's 'ray shock' theory. This theory accurately predicts the results achieved through experiments when the shock strength is weak ($\xi \geqslant 0{\cdot}6$). As the shock strength increases ($\xi < 0{\cdot}6$), the neglection of real-gas effects and the disturbances occurring behind the Mach stem become noticeable. The discrepancies between our theory and the experimental results became greater as ξ decreased.

Locus of triple points – the point of interaction of an incident shock wave, a reflected shock wave, and a Mach stem – were also investigated. Our results, with model *A*, reconfirm Heilig's (1969) experimental results of reflection over a convex wedge. The theoretical locus of triple points is drawn using the method of characteristics (Bryson & Gross 1961) starting at any initial point. The theoretical locus, drawn using the initial point of our calculated critical angles, is in better agreement with the experimental results than that obtained using the initial point obtained with the 'detachment' criterion.

We modified the relation between A and M developed by Milton (1975) using the full Rankine–Hugoniot condition. Using this modified relation between A and M, we developed the theory of the length of Mach stem in Mach reflection over a concave wedge. This theory quite accurately predicts the actual experimental results achieved. Using the theoretical lengths of Mach stem, we can draw the locus of triple points over the concave wedge. We see that the theoretically calculated locus of triple points matches well with the experimental results.

The critical angles of the MR → RR transition obtained by our theory are very close to those found in experiments with weak shock strengths ($\xi \geqslant 0{\cdot}5$). At strong incident shock strengths ($\xi < 0{\cdot}5$), the effects of real gas on the shock motion were more than expected. Additionally, the disturbances which occurred behind the Mach stem deformed the Mach stem. Consequently, further study on the criteria of MR $\rightleftarrows$ RR transition may be necessary at strong incident shock strengths.

The authors would like to express their thanks to Dr W. Heilig of the Ernst Mach Institute, Freiburg, West Germany, Dr L. F. Henderson of the University of Sydney, New South Wales, Australia, and Dr G. Ben-Dor of the Ben-Gurion University of the Negev, Beer Sheva, Israel, for their suggestions. The advice of Dr Takayama of the Institute of High Speed mechanics, Tohoku University, Japan, is also appreciated. Finally we wish to thank Mr R. L. Fullam and Mr M. L. Castell for their assistance in revising this paper for publication in English.

REFERENCES

Ben-Dor G. & Glass, I. I. 1978 *UTIAS Rep.* no. 232.

Ben-Dor, G. & Glass, I. I. 1979 *J. Fluid Mech.* **92**, 3, 459–501.

Ben-Dor, G., Takayama, K. & Kawauchi, T. 1980 *J. Fluid Mech.* **100**, 147–160.

Bryson, A. E. & Gross, R. W. 1961 *J. Fluid Mech.* **10**, 1–16.

Chester, W. 1954 *Phil. Mag.* **45** (7), 1293–1301.

Chisnell, R. F. 1957 *J. Fluid Mech.* **2**, 286–298.

HEILIG, W. 1969 *Physics Fluid Suppl.* **12**, I 154–157.
HENDERSON, L. F. & LOZZI, A. 1975 *J. Fluid Mech.* **68**, 139–155.
HORNUNG, H. G., OERTEL, H. & SANDEMAN, L. 1979 *J. Fluid Mech.* **99**, 541–560.
ITOH, S. & ITAYA, M. 1978 *Japan Soc. Mech. Eng., Paper* no. 408.
KAWAMURA, R. & SAITO, H. 1956 *J. Phys. Soc. Japan* **11**, 538.
MILTON, B. E. 1975 *A.I.A.A. J.* **13**, 1531–1535.
NEUMANN, J. VON 1963 *Collected Works*, vol. 6, pp. 238–299, Pergamon Press.
OSHIMA, K., SUGAYA, K., YAMAMOTO, M. & TOTOKI, T. 1965 *ISAS, University of Tokyo Rep.* no. 393.
SMITH, L. G. 1945 *O. S. R. D. Rep.* no. 6271.
WHITHAM, G. B. 1957 *J. Fluid Mech.* **2**, 145–171.
WHITHAM, G. B. 1958 *J. Fluid Mech.* **4**, 337–360.